

STRAIGHT EDGE EXTRACTION FROM MULTIPLE VIEWS FOR RECONSTRUCTION OF MAN-MADE OBJECTS

Andrew BIBITCHEV

State Research Institute of Aviation Systems, Russia

bibitchev@mail.ru

Working Group III/3

KEY WORDS: buildings, edge extraction, image matching, reconstruction.

ABSTRACT

Man-made object extraction and reconstruction based on edge models are widely used. This paper describes technique of low level extraction of 3D straight edges from multiple views, each of which is gray scale image of 3D scene. The main idea of the approach consists in simultaneous maximization of the following functionals: integral intensity step along 2D line on each image and a special form of correlation between 2D lines on different images, where 2D lines are projections of the 3D edge to appropriate images. During the functionals calculation Gauss pyramids of the images are used, resulting in high speed and stability. Result of maximization is set of 3D edges, i.e. edges in scene space, calculated with sub-pixel accuracy. Moreover, values of the functionals can be treated as weights of appropriate edges in further scene analysis (selection and grouping). Examples of the proposed technique usage for auto and semi-auto building extraction and reconstruction from aerial imagery are included.

1 INTRODUCTION

Although feature extraction is the first serious step to object recognition and image understanding it still remains one of the most complicated problem in computer vision [David M. McKeown, Jr., Chris McGlone, Steven Douglas Cochran, Yuan C. Hsieh, Michel Roux, Jefferey A. Shufelt]. We suppose such situation can be resolved with the aid of maximum prior and input information usage even during low-level stages of image processing and analysis. One of the reasons is following. As a rule there are a number of scene images produced either from different view-points or at different times or in different spectrum parts and we obtain some kind of prior information about dependence between these images. (This paper concerns the first case, i.e. case of different view presence.) At the first analysis stage (low-level analysis) most of the approaches deal with each available view of scene separately, which results in additional data miss. In this paper attempt to use relation between views even during generation of hypothesis is introduced.

The second idea consists in replacing feature extraction task by maximization of functionals, which have integral nature. Thus, we avoid vague threshold selections and complex aggregations. Moreover, as a rule such functionals have sense of feature weight and its values can be used in further analysis. To construct the functionals we can formulate the following characteristics of the features. First of all, feature on image is characterized by special intensity behaviour. Thus, the first functional must describe this behaviour. Let me call it as *integral intensity step functional*. Then, for feature on one image we can try to find appropriate feature on another image. To do this, *special form of correlation* between features on different images is introduced.

For simplicity all aspects, described above, will be discussed for straight edge extraction from gray stereo imagery. Note that generalization is allowed.

This paper is organized as follows. In Section 2 both functionals are constructed and discussed. Also Section 2 concerns the problem of "simultaneous" functionals maximization. In the third Section we consider topics related to proposed feature extraction technique; namely, Gauss pyramid usage during functionals calculation and maximization. In Section 4 application of proposed theory for building extraction and reconstruction is described; moreover, auto and semi-auto approaches are included.

2 ELEMENTS OF THEORY

So, let there exist two images of the one and the same 3d scene. And let shooting geometry be known. We need to extract candidates to 3d straight edges of man-made objects presented in the scene.

2.1 Integral Intensity Step Functional

To begin with, consider construction and usage of integral intensity step functional, i.e. functional, which describes intensity behaviour along straight line.

2.1.1 Heuristic. Let $i(x, y)$ be gray scale discrete image of 3d scene, $x = 0, \dots, s_x - 1$, $y = 0, \dots, s_y - 1$. We need to find

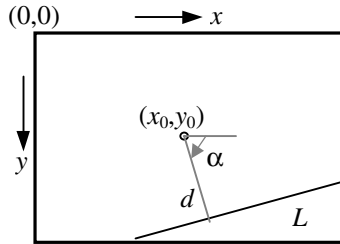


Figure 1. Parametrization

straight intensity steps of function $i(x, y)$, i.e. 2d edges. For convenience, parametrization $\xi = (d, \alpha)$ of straight line L is used:

$$L(d, \alpha) = \{(x, y) \mid (x - x_0) \cos \alpha + (y - y_0) \sin \alpha \approx d\}, \quad (1)$$

$$(d, \alpha) \in \Xi = [-d_{\max}; d_{\max}] \times [0; \pi],$$

where $(x_0, y_0) = (\frac{1}{2}s_x, \frac{1}{2}s_y)$ is center point, $d_{\max} = \frac{1}{2}\sqrt{s_x^2 + s_y^2}$ (see Figure 1).

We propose the following heuristic. Suppose $\mathbf{g} \equiv (g_x, g_y) = |\mathbf{g}| \cdot (\cos \alpha_g, \sin \alpha_g)$ is gradient of intensity $i(x, y)$, then the probability $P(d, \alpha; x, y)$ that point (x, y) belongs to 2d edge $L(d, \alpha)$ is proportional to

$$|\mathbf{g}(x, y)|^{1/q} \cdot \exp\left\{-\frac{\min^2\{|\alpha - \alpha_g|, |\alpha - \alpha_g + \pi|\}}{2\sigma_\alpha^2}\right\}. \quad (2)$$

Here $|\mathbf{g}| = \sqrt{g_x^2 + g_y^2}$ is gradient length; α_g is angle between vector \mathbf{g} and horizontal direction, $\alpha_g \in [0; 2\pi)$; σ_α^2 is constant, which has sense of angle dispersion; $q > 0$ is constant, which defines contribution of high gradient values. For example, if we are interested only in strongly marked 2d edges we should choose $q \ll 1$ and vice versa if we are interested also in watery steps we should choose $q \gg 1$. As to gradient $\mathbf{g}(x, y)$ of intensity $i(x, y)$ its discrete analog can be calculated using convolution with Sobel masks:

$$g_x(x, y) = \begin{pmatrix} -1 & 0 & 1 \\ -2 & 0 & 2 \\ -1 & 0 & 1 \end{pmatrix} * i(x, y), \quad g_y(x, y) = \begin{pmatrix} -1 & -2 & -1 \\ 0 & 0 & 0 \\ 1 & 2 & 1 \end{pmatrix} * i(x, y). \quad (3)$$

The main premise for the proposed heuristic is that in ideal case (no noise, no sampling and no quantization) probability $P(d, \alpha; x, y)$ is proportional to

$$\theta(|\mathbf{g}|) \cdot \delta(\Delta\alpha), \quad (4)$$

where $\Delta\alpha = \min\{|\alpha - \alpha_g|, |\alpha - \alpha_g + \pi|\}$, $\theta(x) = \begin{cases} 1, & x > 0 \\ 0, & x \leq 0 \end{cases}$ is step function and $\delta(x) = \theta'(x)$ is Dirak generalized function. Thus, the first multiplier in expression (2) is weight and corresponds to $\theta(|\mathbf{g}|)$ and the second one is regularized function $\delta(\Delta\alpha)$.

2.1.2 Integral Intensity Step Transform. Using heuristic (2) we can construct the following functional:

$$step(d, \alpha) = \sum_{(x,y) \in L(d,\alpha)} P(d, \alpha; x, y) = \sum_{(x-x_0) \cos \alpha + (y-y_0) \sin \alpha = d} |\mathbf{g}(x, y)|^{1/q} \exp \left[-\frac{\min^2 \{ |\alpha - \alpha_g|, |\alpha - \alpha_g + \pi| \}}{2\sigma_\alpha^2} \right]. \quad (5)$$

This functional has sense of integral intensity step along straight line $L(d, \alpha)$. Note that expression (5) for $(d, \alpha) \in \Xi$ defines transform of image $i(x, y)$.

In practice to compute values of $step(d, \alpha)$ we can use voting method applied for Hough transform calculation. Namely, first of all discrete grid with steps $\Delta d = 1$ and $\Delta \alpha = \frac{1}{2d_{\max}}$ is introduced in area Ξ of parameters values; then, the following algorithm is performed:

1. put $step(d, \alpha) \equiv 0$;
2. for each point (x, y) of source image do steps 3 ÷ 6:
3. calculate $\mathbf{g}(x, y)$ using Sobel operator (3); calculate $|\mathbf{g}|^{1/q}$, α_g ;
4. for each discrete value of α such that $\min \{ |\alpha - \alpha_g|, |\alpha - \alpha_g + \pi| \} < 3\sigma_\alpha$ do steps 5 ÷ 6:
5. assign the nearest discrete value of $(x - x_0) \cos \alpha + (y - y_0) \sin \alpha$ to d ;
6. add $P(d, \alpha; x, y)$ to $step(d, \alpha)$.

Note that to improve the algorithm performance fixed point mathematics and precalculated tables of functions can be used. Moreover, in section 3 application of Gauss pyramids, that result in speed and stability gain, will be discussed.

In Figure 2 you can see the results of the integral transform (5) for fragment of aerial image. To obtain this results, constants q and σ_α were assigned to 4 and 0.1 respectively.

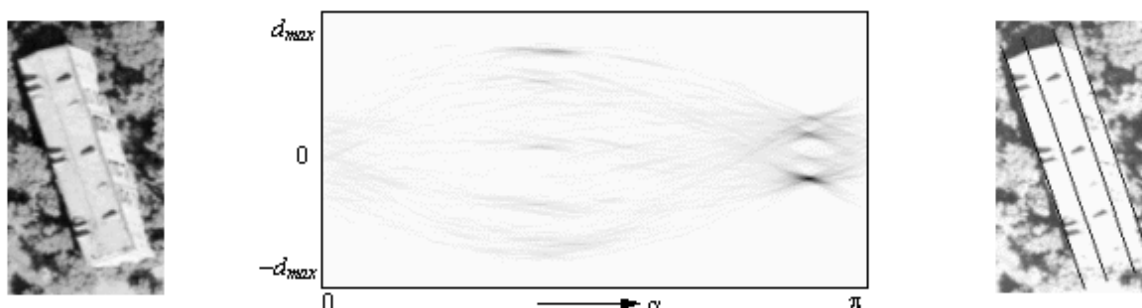


Figure 2. Example of integral intensity step transform: source image (at the left), result of transform (at the center) and extracted edges (at the right)

2.1.3 Finding of Candidates to 2d Edges. Due to form of functional (5) its local maximums have strongly marked form (see Figure 2). These local maximums should be treated as candidates to 2d edges. The following procedure can be applied for candidates choosing. First of all we find global maximum of $step(d, \alpha)$, let me denote it as (d_1, α_1) , i.e. candidate number 1. Then we exclude vicinity (e.g. 5×5) of point (d_1, α_1) and find new global maximum in the rest of the grid, as a result (d_2, α_2) will be obtained. And so on. There is one question: when should we stop it? The answer depends. For example, if we need to find N 2d edges, it is reasonable to test first kN candidates, where $k > 1$.

Note that when we define vicinity of point (d_i, α_i) we must remember that $\xi = (d, \alpha)$ is toroidal coordinates, that is $(d, 0)$ is equivalent to $(-d, \pi)$ for any d .

2.1.4 Contour Ends Extraction. Let us remark that detection of contour ends remains serious problem. To resolve this problem, one can use Forstner operator [W. Eckstein, 1996] or various corner detectors [A. Singh, M. Shneier, 1989]. But all known operators of such type have low robustness. For this reason we prefer to solve problem of end detection via intersection of contours.

2.1.5 Advantages and Drawbacks. Among advantages of described technique the following ones can be accentuated:

- high robustness;
- high tolerance, i.e. edge can be not exactly straight;
- $step(d, \alpha)$ can be treated as weight of $L(d, \alpha)$;
- generalization is allowed, i.e. one can construct functional $step$ for any parametrized curve.

But the following drawbacks take place:

- $step(d, \alpha)$ is useful only for detection of contours with length comparable with image size, thus we must know interest area for edge searching rather well;
- additional efforts are required to determine the end-points.

2.2 Correlation of 2d Edges

To enter the second part of desired functional let me consider the following auxiliary task.

2.2.1 Auxiliary Task. Suppose there are two different gray scale images of one and the same 3d scene: $i^S(x^S, y^S)$ is “source” image of size $s_x^S \times s_y^S$ and $i^D(x^D, y^D)$ is “destination” image of size $s_x^D \times s_y^D$. Furthermore, parameters of internal, relative and optionally external orientation are assumed to be known, that is 2d image coordinates can be transformed in 3d scene coordinates (X, Y, Z) and vice versa:

$$X = X(x^S, y^S; x^D, y^D), Y = Y(x^S, y^S; x^D, y^D), Z = Z(x^S, y^S; x^D, y^D); \tag{6}$$

$$x^S = x^S(X, Y, Z), y^S = y^S(X, Y, Z); \tag{7}$$

$$x^D = x^D(X, Y, Z), y^D = y^D(X, Y, Z). \tag{8}$$

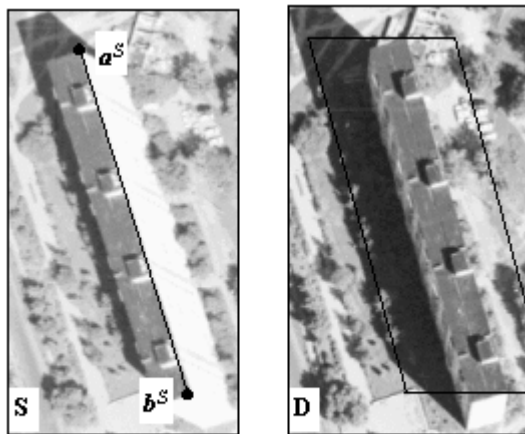


Figure 3. “Source” (at the left) and “destination” (at the right) images of 3d scene

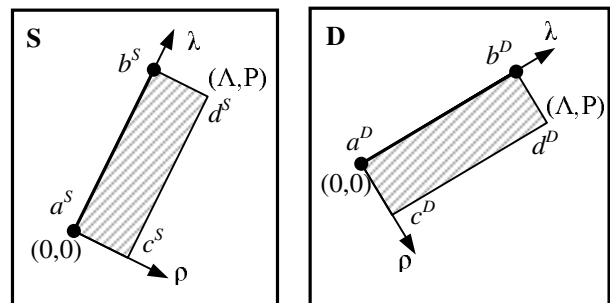


Figure 4. Coordinate system in vicinities

And let we have 2d edge $a^S b^S$ on the “source” image (see Figure 3). We need to match 2d edge $a^D b^D$ on the “destination” image, that is we need to find $a^D b^D$ such that $a^S b^S$ and $a^D b^D$ are projections of one and the same 3d scene edge AB on “source” and “destination” images respectively.

To include (by indirection) 3d object model, we can require that there is parametrization ω of all possible AB positions:

$$A = A(a^S, b^S; \omega), B = B(a^S, b^S; \omega), \omega \in \Omega, \tag{9}$$

and thus

$$a^D = a^D(a^S, b^S; \omega), b^D = b^D(a^S, b^S; \omega), \omega \in \Omega. \tag{10}$$

For example, in case of edges of flat horizontal building roof height coordinate H can be considered as parameter ω , moreover bounds H_{\min} and H_{\max} define set $\Omega: \Omega = [H_{\min}; H_{\max}]$.

Thereby, the task can be reformulated as follows. It is required to find value of parameters ω from set Ω , for which $a^S b^S$ and $a^D b^D$ are projections of one and the same 3d edge AB on “source” and “destination” images respectively.

2.2.2 Correlation. Obviously, for matched 2d edges $a^S b^S$ and $a^D b^D$ their (one-side) vicinities on images are cognate to each other. Thus, to match $a^S b^S$ and $a^D b^D$, similarity of their (one-side) vicinities as a function of ω should be maximized on the set Ω . Note that one-side vicinity usage is preferable due to existence of application noise. As an example, in Figure 3 we can see right building wall in the “source” image and can not in the “destination” one.

Let $V^S = a^S b^S c^S d^S$ be vicinity of $a^S b^S$ and $V^D = a^D b^D c^D d^D$ be appropriate vicinity of $a^D b^D$. Note that dependence $V^D = V^D(V^S; \omega)$ should include 3d model of object facets. To construct measure of similarity, let me introduce coordinates (λ, ρ) presented in Figure 4, here Λ is $a^S b^S$ length in pixels and P is vicinity width in pixels. Then, the normalized correlation coefficient of vicinities can be introduced:

$$corr(a^S, b^S; \omega) = \begin{cases} -1, & i^S \equiv const \text{ or } i^D \equiv const \\ \frac{i^S(\lambda, \rho) i^D(\lambda, \rho) - \overline{i^S(\lambda, \rho)} \cdot \overline{i^D(\lambda, \rho)}}{\sqrt{\left[\overline{(i^S(\lambda, \rho))^2} - \overline{i^S(\lambda, \rho)}^2 \right] \cdot \left[\overline{(i^D(\lambda, \rho))^2} - \overline{i^D(\lambda, \rho)}^2 \right]}}, & \end{cases} \quad (11)$$

where $i^S(\lambda, \rho) = i^S(x^S(\lambda, \rho), y^S(\lambda, \rho))$ is “source” image in new coordinates, $i^D(\lambda, \rho) = i^D(x^D(\lambda, \rho; \omega), y^D(\lambda, \rho; \omega))$ is “destination” image in new coordinates, and $\overline{f(\lambda, \rho)} = \frac{1}{(\Lambda+1) \cdot P} \sum_{\lambda=0}^{\Lambda} \sum_{\rho=1}^P f(\lambda, \rho)$ is mean value of a function $f(\lambda, \rho)$. For calculation intensities i^S and i^D at points with non-integer coordinates one can use bilinear interpolation.

As well known coefficient (11) has following useful properties:

- (i) $-1 \leq corr \leq 1$;
- (ii) $corr = 1 \Rightarrow i^S(\lambda, \rho) \equiv k i^D(\lambda, \rho) + c$, where k and c are constants;
- (iii) $corr$ is invariant for linear intensity transformations $i' = k i + c$.

All these properties allow us to consider matching problem as optimization task:

$$\omega^* = \arg \max_{\omega \in \Omega} corr(a^S, b^S; \omega), \quad (12)$$

$$a^D = a^D(a^S, b^S; \omega^*), b^D = b^D(a^S, b^S; \omega^*). \quad (13)$$

If $corr(a^S, b^S; \omega^*)$ less than threshold value (usually 0.3) then candidate $a^S b^S$ should be rejected.

Example of correlation results for two candidates to the long sides of the building roof, imaged in Figure 3, is presented in Figure 5. It is easy to see that for both edges we obtain one and the same value of height: $H^* = 192$ m.

2.2.3 Advantages and Drawbacks. Let me enumerate some advantages of such correlation usage:

- high robustness;

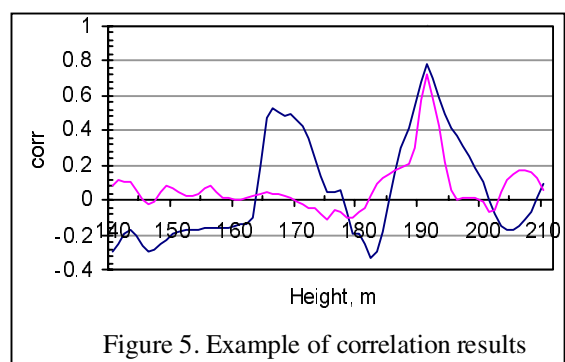


Figure 5. Example of correlation results

- subpixel accuracy;
- absence of vague thresholds.

Also, there is serious disadvantage – rather high calculation cost. To eliminate this drawback Gauss pyramid can be used (see Section 3).

2.3 Fusion Of Integral Intensity Step And Correlation

Let $step^S(d^S, \alpha^S)$ be integral step transform of the “source” image $i^S(x^S, y^S)$; $step^D(d^D, \alpha^D)$ be integral step transform of the “destination” image $i^D(x^D, y^D)$; $\{(d_i^S, \alpha_i^S)\}_{i=1}^N$ be selected local maximums of $step^S(d^S, \alpha^S)$; $\{a_{ij}^S b_{ij}^S\}_{j=1}^{K_i}$ be conjectural end points of 2d edge $L(d_i^S, \alpha_i^S)$. To obtain set of 3d edges $\{A_i B_i\}$ one can apply the following procedure:

1. For each $i=1, \dots, N$ and each $j=1, \dots, K_i$ we perform maximization

$$W_{ij}(d^S, \alpha^S; \omega) = [step^S(d^S, \alpha^S) + step^D(d^D(d^S, \alpha^S; \omega), \alpha^D(d^S, \alpha^S; \omega))] \cdot corr(\Pr_{L^S(d^S, \alpha^S)} a_{ij}^S, \Pr_{L^S(d^S, \alpha^S)} b_{ij}^S; \omega) \rightarrow \max$$

with restrictions $|d^S - d_i^S| \leq 2\Delta d^S, |\alpha^S - \alpha_i^S| \leq 2\Delta \alpha^S, \omega \in \Omega.$ (14)

Here $\Pr_L p$ is projection of point p on line L . As a result we obtain $\tilde{d}_{ij}^S, \tilde{\alpha}_{ij}^S, \omega_{ij}^*$ and $\tilde{\alpha}_{ij}^S = \Pr_{L^S(\tilde{d}_{ij}^S, \tilde{\alpha}_{ij}^S)} a_{ij}^S, \tilde{b}_{ij}^S = \Pr_{L^S(\tilde{d}_{ij}^S, \tilde{\alpha}_{ij}^S)} b_{ij}^S$.

2. For each $i=1, \dots, N$ we choose j with maximum value of $W_{ij}(\tilde{d}_{ij}^S, \tilde{\alpha}_{ij}^S; \omega_{ij}^*)$. Let me denote such j as j_i^* .
3. After all, we can calculate 3d edges:

$$A_i = A(\tilde{\alpha}_{ij_i^*}^S, \tilde{b}_{ij_i^*}^S; \omega_{ij_i^*}^*), B_i = B(\tilde{\alpha}_{ij_i^*}^S, \tilde{b}_{ij_i^*}^S; \omega_{ij_i^*}^*), i = 1, \dots, N. \tag{15}$$

Note that weight of $A_i B_i$ is $W_i = W_{ij_i^*}(\tilde{d}_{ij_i^*}^S, \tilde{\alpha}_{ij_i^*}^S; \omega_{ij_i^*}^*)$.

3 GAUSS PYRAMID USAGE

Here we want to say a few words about related topic, namely Gauss pyramid usage for fast and robust calculation. It should be noted that application of Gauss pyramid allows one to construct scale-independent algorithms [Poul S. Wu, Ming L., 1997].

Let $\{i_l^S(x, y)\}_{l=0}^L$ be Gauss pyramid of the “source” image: $i_0^S \equiv i^S$ is the bottom level of pyramid, i_L^S is the top level, $(s_x^S)_l = \lfloor \frac{1}{2}(s_x^S)_{l-1} \rfloor$ and $(s_y^S)_l = \lfloor \frac{1}{2}(s_y^S)_{l-1} \rfloor, l = 1, \dots, L$. And let $\{i_l^D(x, y)\}_{l=0}^L$ be appropriate Gauss pyramid of the “destination” image. The count of layers $L+1$ should be chosen so that character size of the object on the top level images i_L^S and i_L^D is not less than several pixels. Note that in practice $L-1$ is usually equal to $2 \div 4$.

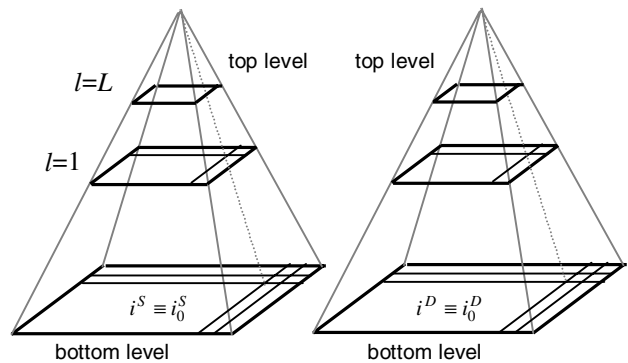


Figure 6. Gauss pyramids of “source” and “destination” images

As soon as we construct Gauss pyramids we can apply the technique described in previous section to top-level images i_L^S and i_L^D . As a result we obtain set of 3d edges $\{A_i^L B_i^L\}_{i=1}^N$. Then, these 3d edges we use to construct predictions for the lower layers:

$$(a_i^S)_{L-1} = (a^S)_{L-1}(A_i^L, B_i^L), (b_i^S)_{L-1} = (b^S)_{L-1}(A_i^L, B_i^L), \tag{16}$$

$$(a_i^D)_{L-1} = (a^D)_{L-1}(A_i^L, B_i^L), (b_i^D)_{L-1} = (b^D)_{L-1}(A_i^L, B_i^L). \quad (17)$$

Therefore on layer $L-1$ of the pyramid maximization (14) can be performed only in vicinities of 2d edges $(a_i^S)_{L-1}(b_i^S)_{L-1}$ and $(a_i^D)_{L-1}(b_i^D)_{L-1}$, that allow us to decrease area of search radically. As a result we obtain set of 3d edges $\{A_i^{L-1} B_i^{L-1}\}_{i=1}^N$. And so on until bottom level of the pyramid will be reached.

Due to Gauss pyramid application the speed of the algorithm goes up in times.

4 APPLICATION EXAMPLES

Initially, proposed technique was developed for building extraction from aerial imagery. For this reason application examples are auto and semi-auto buildings extraction.

Available input data is:

- stereo-pair of gray scale aerial images;
- parameters of internal, relative and external orientations;
- some parameters of buildings (minimum and maximum height, minimum and maximum length of short side and so on);
- DEM produced by stereo-correlation procedure (optionally).

Required output data is:

- 3d digital models of building roofs;
- DEM of ground (optionally).

4.1 Semi-Auto Building Extraction

The main idea of semi-auto approach consists in the following. User performs only supervisor functions, and the computer does all stale and accurate operations. The approach scheme is presented in Figure 7.

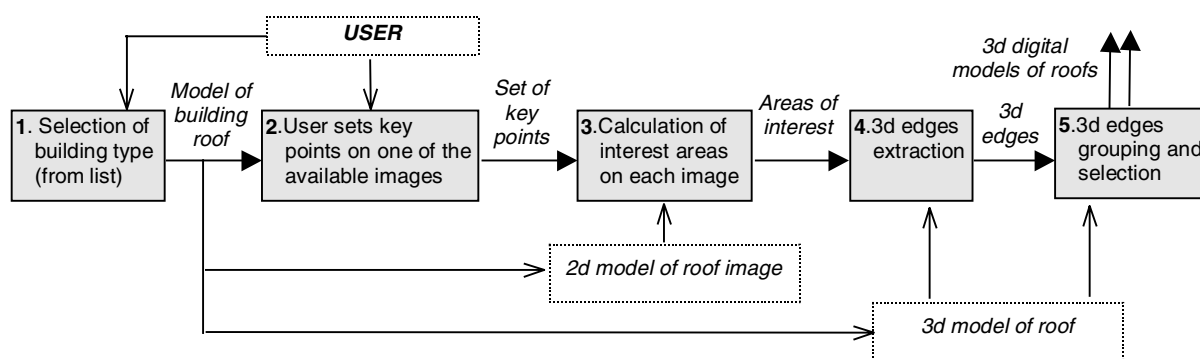


Figure 7. Scheme of semi-auto building extraction procedure

First of all user must select type of the building. For each building type appropriate model is supposed to be known. Then, user must mark on any image rough position of key points. Key point selection is some kind of “know how” and depends on building type. For example, in case of rectangle flat roof we can use two key points: one arbitrary point on each short side of the roof image. Next, using marked positions of key points we can produce areas of interest on each available image. In these areas algorithm of 3d edge extraction is run. As result we obtain candidates to roof sides. Using key points and 3d relational model of the roof selection and grouping of 3d edges are performed. Thus, we obtain a number of roof hypotheses. The hypothesis with maximum total weight is selected as a final result of reconstruction. Note that total weight of roof hypothesis must include as weights of 3d edges constituting roof as measure of adequacy to the model.

Described approach is used commercial Win32 application “Simple Building Extraction”, which allows easy and fast create accurate 3d digital models of cities and towns.

4.2 Auto Building Extraction

If we have detailed DEM produced by stereo-correlation procedure, then we can try to use the DEM for definition of interest areas.

First of all DEM of the ground can be calculated with the aid of dual-rang filter [W. Eckstein, 1996]. Then, difference between initial DEM and filtered DEM is used to localize high objects, such as trees, buildings and so on. This allows us to obtain areas of interest on the images. However, there are two problems. First calculation of detailed DEM requires a lot of time and resources. Secondly separation of interest area for one object from interest area for another object is often problematic (due to existence of trees and neighbouring buildings).

Nevertheless, as soon as we produce areas of interest we can perform steps 4 and 5 of semi-auto algorithm.



Figure 8. Example of building reconstruction: left image of stereo-pair with extracted roof edges (at the left), right image of stereo-pair with extracted roof edges (at the center) and reconstructed 3d model (at the right)

5 CONCLUSION

It was shown that 3d features extraction can be performed via maximization of two functionals: integral intensity step along 2d edge and correlation between 2d edges on different images. Proposed approach is used in applications and has proved its advantages. Future work is supposed to be concerned with complicated models of buildings and development of model's pyramids.

ACKNOWLEDGEMENTS

I would like to thank S. Zheltov and U. Blokhinov for their valuable suggestions and supporting.

REFERENCES

- David M. McKeown, Jr., Chris McGlone, Steven Douglas Cochran, Yuan C. Hsieh, Michel Roux, Jefferey A. Shufelt. Automatic Cartographic Feature Extraction Using Photogrammetric Principles. Manual of Photogrammetry Addendum, Chapter 9: Feature Extraction and Object Recognition
- A. Singh, M. Shneier, 1989. Grey Level Corner Detection: A Generalization and a Robust Real Time Implementation. Computer Vision, Graphics, And Image Processing 51, 54-69 (1990)
- Poul S. Wu, Ming L., 1997. Pyramid Adaptive Dynamic Hough transform to detect edges with arbitrary shapes. Opt. Eng. 36(5), Society of Photo-optical Instrumentation Engineers
- W. Eckstein, 1996. Segmentation and Texture Analysis. International Archives of Photogrammetry and Remote Sensing. Vol. XXXI, Part B3.